Velocity Models from Three-Dimensional Traveltime Tomography in the Nechako Basin, South-Central British Columbia (Parts of NTS 093B, C, F, G)

D.A. Talinga, Simon Fraser University, Burnaby, BC, dtalinga@sfu.ca

A.J. Calvert, Simon Fraser University, Burnaby, BC

Talinga, D.A. and Calvert, A.J. (2011): Velocity models from three-dimensional traveltime tomography in the Nechako Basin, south-central British Columbia (parts of NTS 093B, C, F, G); *in* Geoscience BC Summary of Activities 2010, Geoscience BC, Report 2011-1, p. 265–274.

Introduction

The Nechako Basin is located in the interior plateau of British Columbia, and is bounded to the east by the Rocky Mountains and to the west by the Coast Mountains (Figure 1; Hayes and Fattahi, 2002; Calvert and Hayward, 2009). Although the basin has been an occasional exploration target since the first well was drilled in 1931, the complex tectonic history and challenges associated with imaging inside and below volcanic sequences prevented a good understanding of its architecture and hydrocarbon potential (Calvert and Hayward, 2009). Past drilling attempts by Honolulu Oil Corporation Limited, Hudson's Bay Oil and Gas Company Limited and Canadian Hunter Exploration Limited, which documented the presence of oil, asphalt and gas anomalies in wellbores (Hannigan et al., 1994; Hayes and Fattahi, 2002; Ferri and Riddell, 2006), and recent results of a hydrocarbon-potential evaluation of the basin (Riddell, 2009) suggest that the south-central part of the basin is the most prospective, with structural trapping elements and potential Cretaceous and Jurassic sources and reservoirs.

The 2008 Geoscience BC seismic survey consists of seven two-dimensional (2-D) crooked lines acquired in the east-central part of the basin (Figure 2), with one of the goals being to map the extent of the outcropping Early Cretaceous rocks in order to determine if they were deposited within a single large basin or within several sub-basins (Calvert and Hayward, 2009). The Cretaceous rocks in this area are of particular interest for exploration because they contain all the hydrocarbon shows identified in the Canadian Hunter wells (Calvert and Hayward, 2009). In addition, these rocks could provide structural traps resulting from the development of compressional folds and drag folds (Hannigan et al., 1994).

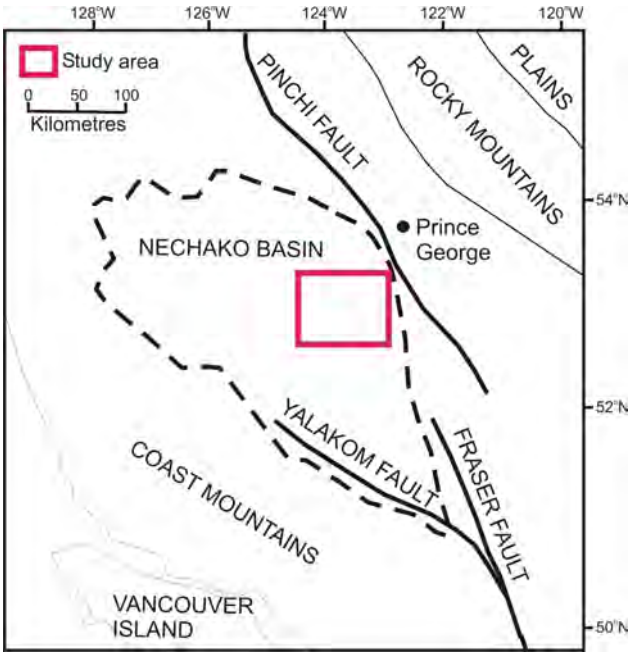

Figure 1. Location of the Nechako Basin in south-central British Columbia and approximate position of the study area in the east-central part of the basin.

In this paper we present velocity models obtained from three-dimensional (3-D) tomographic inversion of refracted waves recorded on two of the Geoscience BC seismic lines:

east-trending line 2008-15, shot across Tertiary deposits comprising volcanic rocks of the Eocene Endako Group and Ootsa Lake Group

roughly east-trending line 2008-11, shot mainly across upper Tertiary volcanic rocks of the Chilcotin Group but with Quaternary cover to the east and outcropping Cretaceous volcanic rocks to the west (see Figure 2)

Overcoming Challenges in Imaging Subvolcanic Structures

Because of the layered nature of the volcanic sequences, which in some locations are more than 1000 m thick (Hannigan et al., 1994), one of the major problems in the

Keywords: *Nechako Basin, hydrocarbon exploration, three-dimensional seismic tomography, imaging, volcanic cover, velocity models*

This publication is also available, free of charge, as colour digital files in Adobe Acrobat® PDF format from the Geoscience BC website: http://www.geosciencebc.com/s/DataReleases.asp.

Nechako Basin is imaging subvolcanic structures. Previous studies in volcanic environments identify these main challenges in seismic imaging:

Large impedance contrasts occur at the top and base of individual volcanic sequences. At near-vertical incidence, almost no energy can penetrate the volcanic layers, whereas, at wide angles, it is difficult to recover velocity information if the underlying sedimentary sequences have a lower velocity than that of the basalt, because no turning waves are created in the low-velocity units (Fliedner et al., 1998).

Complex interference effects result from the alternation of volcanic and sedimentary sequences, which distort or obscure reflections from below the volcanic units (Lafond et al., 1999).

Scattering caused by the rugged interfaces of the basalt layers and lateral heterogeneity within the basalt sequence can all cause the attenuation of seismic waves, resulting in the poor continuity and low amplitude of primary reflections (Lafond et al., 1999).

The main objective of the Geoscience BC seismic survey was to improve the current geological knowledge of the area by imaging the data in the optimal way, based on the nature of the environment (Calvert et al., 2009). The quality of previously recorded seismic data in the area indicates that the presence of volcanic rocks in the near surface may contribute to the absence of refracted arrivals by causing poor source-to-ground coupling of vibroseis sources, and also of continuous reflections on the final seismic sections.

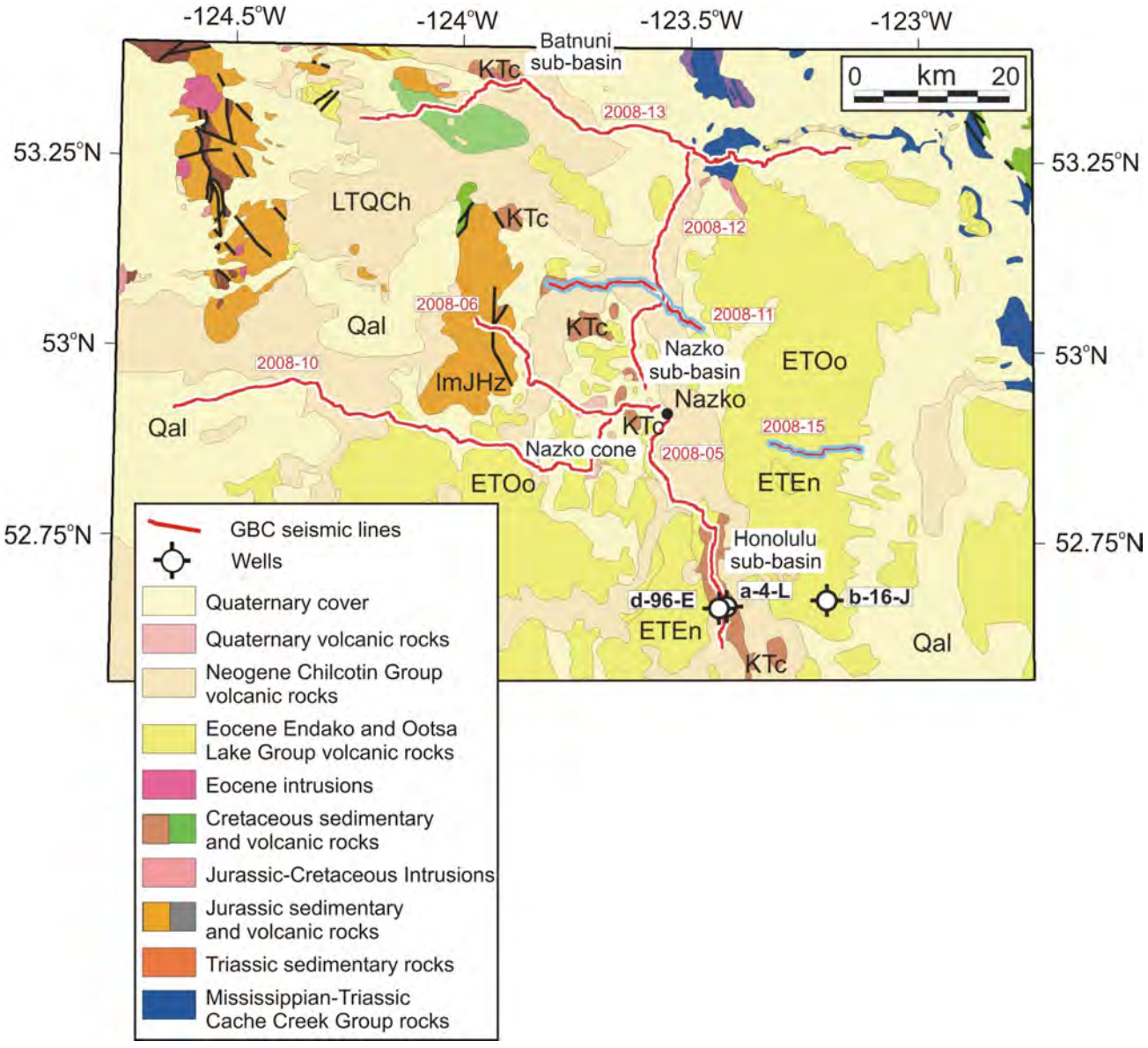

Figure 2. Location of Geoscience BC seismic survey and surface geology, south-central British Columbia; this paper focuses on lines 2008-15 and 2008-11 (highlighted in blue).

Therefore, the Geoscience BC seismic survey was designed to improve the signal-to-noise ratio through use of the following criteria (Calvert and Hayward, 2009):

- longer offsets (maximum 14390 m) to record deep subvolcanic reflections and refraction arrivals to resolve the thickness of the surface volcanic layer
- low-frequency sweeping (8–64 Hz) to improve transmission through the shallow volcanic layer, since energy passing through the basalt is strongly attenuated at frequencies above 30 Hz
- use of a large array of vibrators (four) with long sweeps (28 seconds) to maximize the source strength

Velocity Structure from Three-Dimensional Refraction Tomography

The goal of seismic tomography is to make geological deductions from indirect and often noisy seismic observations. In the Nechako Basin, the volcanic rocks in the near surface impede imaging of underlying structures and consequently interfere with estimation of hydrocarbon potential, which is closely related to the shape of the structures. Previous studies in basaltic environments suggest that using traveltime tomography and long-offset seismic data has the potential to improve the structural definition of subbasalt structures.

In the Nechako Basin, 2-D first-arrival tomographic velocity modelling has been used by Hayward and Calvert (2009) on the Canadian Hunter data to examine shallow structures situated south of the Geoscience BC seismic survey. However, use of 2-D refraction tomography is inadequate with the newly acquired data because of crooked-line geometry and strong velocity variations in the subsurface, both of which have the potential to produce significant out-of-plane ray bending and hence velocity artifacts in the inversion.

The 3-D velocity structure for the two crooked seismic lines analyzed (total of 39.5 km) was obtained using the First Arrival Seismic Tomography program (FAST), which is based on the regularized tomographic method (Zelt and Barton, 1998). The algorithm inverts first-arrival traveltimes to find a geologically reasonable velocity model with a minimum amount of structure. The final model is considered minimum-velocity structure if it is very close to the starting model (Zelt and Barton, 1998). The forward calculation of traveltimes, ray paths and model update uses a 3-D velocity-model parameterization with a uniform node spacing, and the calculation is based on the 3-D finite-difference solution of Vidale (1990) to the eikonal equation. The method was adapted by Hole and Zelt (1995) to handle large velocity gradients or contrasts.

Inversion of the traveltimes is a nonlinear problem because the ray paths are velocity dependent and unknown (Zelt et al., 2006). The nonlinearity is typically resolved by repeated application of linearized inversion and constraints to the data through a process called regularization (Zelt and Barton, 1998). The inverse problem is solved so that the data are fit according to their assigned uncertainties while solving for the model parameters that satisfy two structure constraints: *lambda*, which controls the long-wavelength structure in the initial iterations and allows short-wavelength structure in later iterations (Zelt et al., 2006); and *sz,* which is the ratio of vertical and horizontal smoothing/flatness.

Starting Velocity Models

In general, the stratigraphy, velocity and depth structure of the Nechako Basin are not well known, principally due to insufficient and poor-quality seismic data. Because there was no prior information concerning the velocity structure in the study area, we used several one-dimensional starting models to evaluate the differences between the observed times of first arrivals (manually picked on both seismic lines) and first arrivals estimated for each initial test model.

The topography was incorporated into the starting models for both lines 2008-15 and 2008-11, with a fixed overlying starting velocity of 1.5 km/s to reduce artifacts due to the large velocity contrast across the surface interface. The preferred starting models had surface velocities of 3.3 km/s at 1400 m elevation for line 15, and 3.1 km/s at 1100 m elevation for line 11. The velocity gradient for both seismic lines was 0.9 s^{-1}. Table 1 summarizes the initial velocity models for the two seismic lines.

The vertical/horizontal smoothness constraint parameter *sz* was chosen to be 0.2, while the starting value for *lambda* was 100. Seven *lambda* values were tested for each nonlinear iteration, each value decreasing by a factor of about 1.41.

Recovered Velocity Models

For line 2008-15, the model was defined on a 0.05 km grid extending from –1.5 to 14.9 km in the x direction, –3.4 to 1.5 km in the y direction, and –2.0 to 3.5 km in the z direction. The elevation along the line varies from –1355 to –1117 m above mean sea level, and the location of the origin corresponds to the westernmost shot of the line. After seven iterations of the linearized inversion, the root-mean-square (RMS) traveltime misfit was 20 ms. Velocities modelled

Table 1. Summary of the starting velocity models for the tomographic inversion of lines 2008-15 and 2008-11 from the Geoscience BC seismic survey, south-central British Columbia.

Seismic line	Surface velocity (km/s)	Elevation of surface velocity (m)	Velocity gradient (s^{-1})
2008-15	3.3	1400	0.9
2008-11	3.1	1100	0.9

from the tomographic inversion are shown in Figure 3; near the surface, the velocity model is characterized by low velocities (approximately 2.6 km/s) in the west and east. Horizontal velocity slices (Figure 4) show that higher velocities (approximately 3.5 km/s) are present in the central part of the model within 900 m of the surface. The decrease in velocity at the extremities of the line does not coincide with the known surface geology, which indicates only lower Tertiary volcanic rocks from the Endako and Ootsa Lake groups, which are expected to have seismic velocities in the 3.5–4.0 km/s range. The ray coverage along the seismic line (Figure 5) shows rays penetrating approximately 2 km below the surface, but overall the data are not well constrained below 800 m from the surface due to the drop in ray density. The depth of ray penetration depends on the maximum source and receiver offset and on the subsurface geology, with the seismic waves propagating preferentially through layers with a low velocity gradient. Two 'shadow' areas with no ray hits are identified along the line. One is between 7 and 9.5 km, from –0.5 to 0.5 km depth, and corresponds to a change in the line direction from east to south and back to east. The other occurs between 4 and 8.5 km for approximately 500 m from the surface. A comparison with the modelled velocities indicates that areas with a high density of rays tend to correspond to local high-velocity anomalies.

The 3-D velocity model for line 2008-11 extends from –1.5 to 23.9 km in the x direction, –8.5 to 1.5 km in the y direction, and –1.6 to 3.5 km in the z direction. The location of the origin corresponds to the westernmost shot, and the elevation along the line varies from –1024 to –827 m. The velocity structure obtained after seven iterations is shown in Figure 6, with an RMS traveltime residual of 38 ms. Eastern and western portions of the line have low velocity values of approximately 2.5 km/s, whereas the central part has high velocity values of 3.5 km/s. This trend is observed in the horizontal velocity slices at 100 m intervals (Figure 7) only at shallow depths, namely in the first 200 m interval. The surface geology map indicates that the middle part of the line was shot across upper Tertiary volcanic rocks from the Chilcotin Group; the eastern part across Quaternary deposits, usually comprising glacial deposits; and the western part across Cretaceous clastic rocks, mainly sandstone. At depths greater than 200 m, the trend reverses: the highest velocities occur to the east and west, and the lowest velocity is in the central part of the line. This trend is most evident on the –0.4 km velocity slice, which indicates velocities in the 4.5–5.0 km/s range for the eastern and west parts, and in the 3.5–4.0 km/s range for the central part. The ray-density map (Figure 8) along the line shows rays penetrating 3.5 km below surface but with a generally nonuniform and reduced coverage. An extended area of zero ray density in the near surface between 11 and 18 km corresponds to a change in the line orientation from east to southeast. The ray coverage along the line is an indication that the resolution of the velocity model along the line is variable.

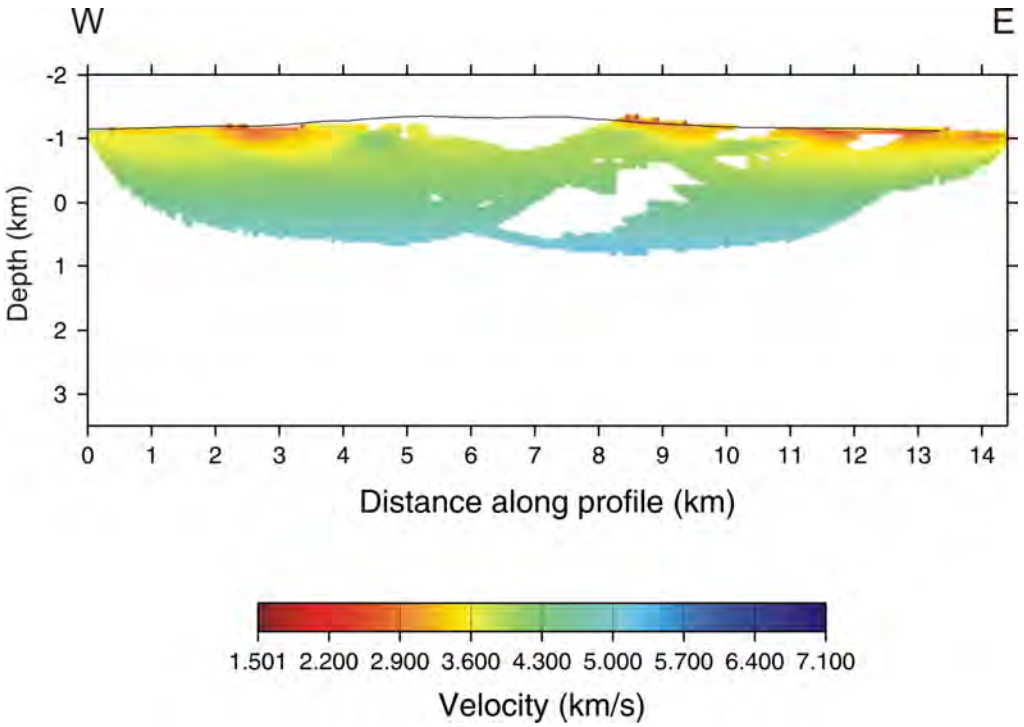

Figure 3. Tomographic velocity model for line 2008-15, characterized in general by smooth structures. Depths are measured relative to mean sea level. The x-axis origin (0) corresponds to the westernmost shot of the line.

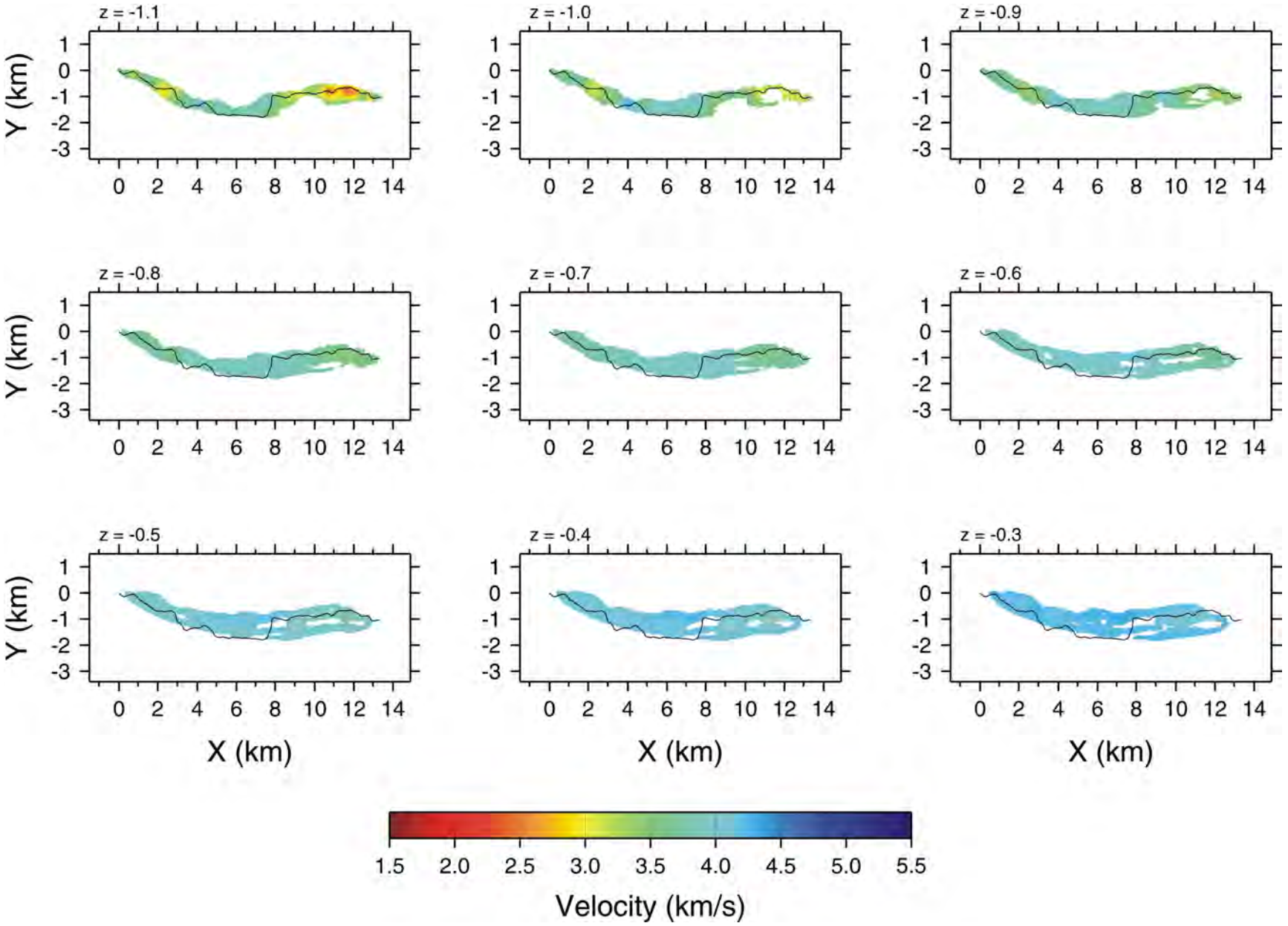

Figure **4.** Horizontal slices of the velocity model for line 2008-15 at depth intervals of 100 m, showing mostly large-scale velocity anomalies. The top left slice is from the shallowest depth and the bottom right slice is from the deepest depth.

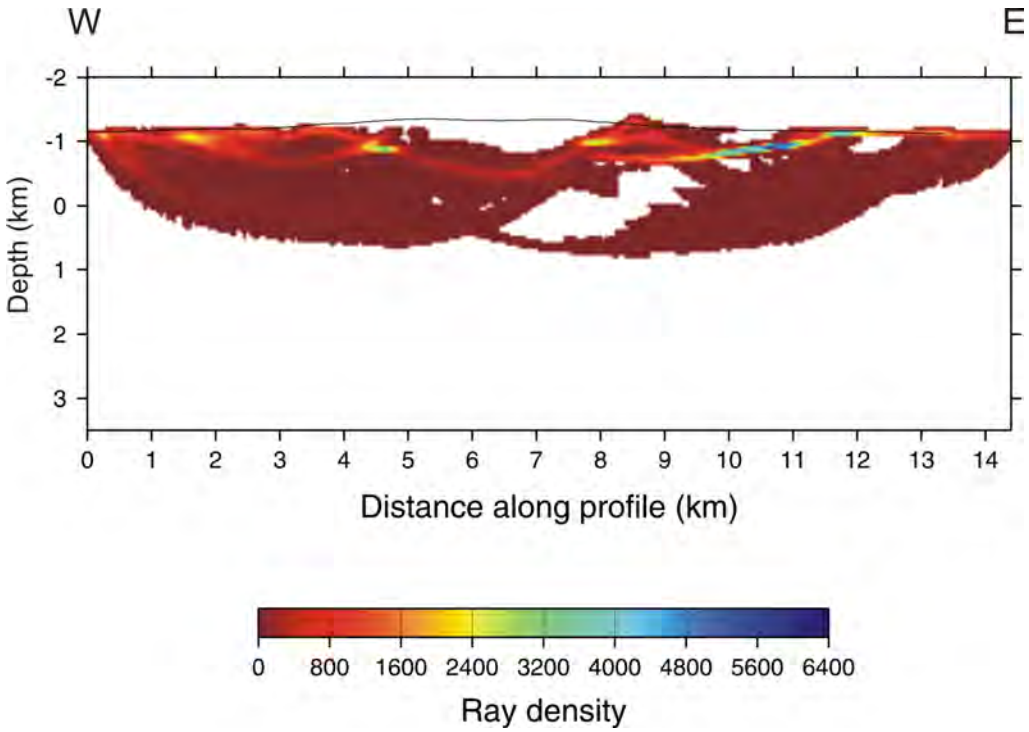

Figure 5. Ray density along line 2008-15, showing rays penetrating 2.0 km below the surface. Highly focused areas of rays have been mapped into local high-velocity anomalies in the recovered velocity model. Depths are measured relative to mean sea level.

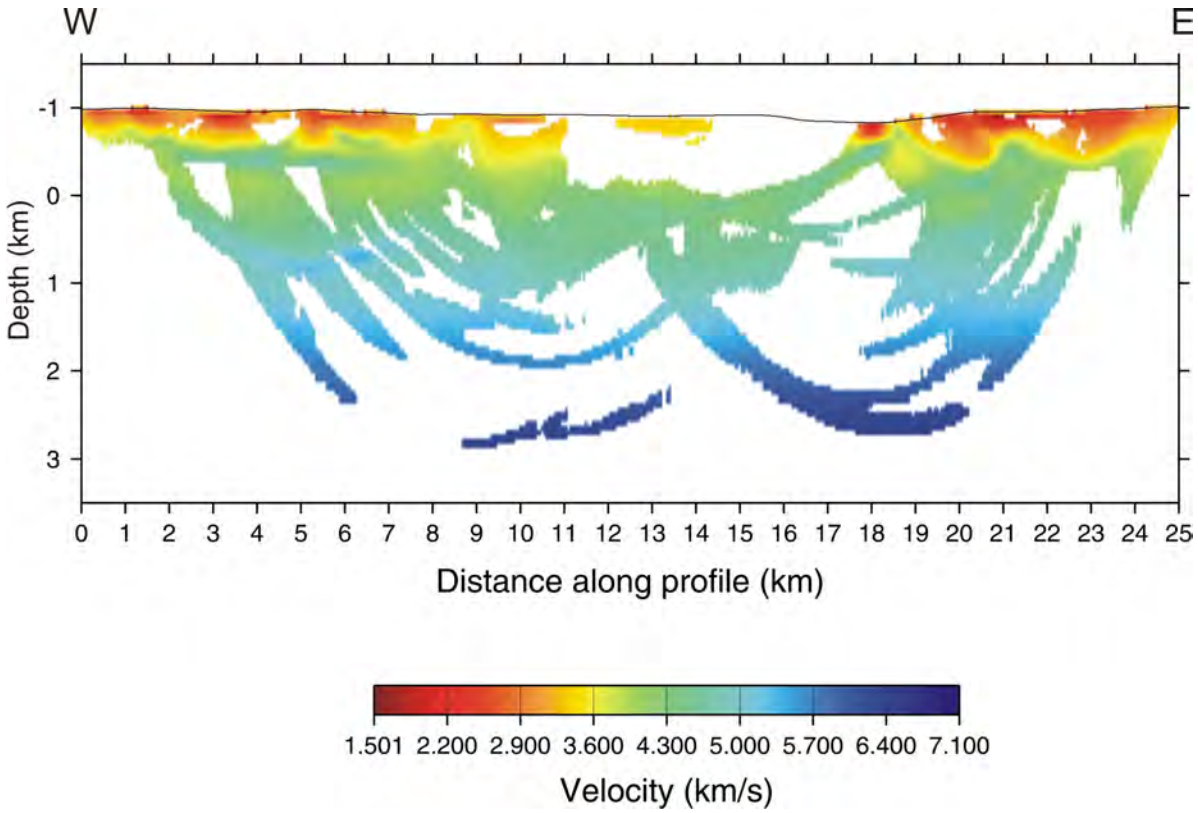

Figure 6. Tomographic velocity model for line 2008-11, showing a heterogeneous shallow section. Depths are measured relative to mean sea level. The x-axis origin (0) corresponds to the westernmost shot of the line.

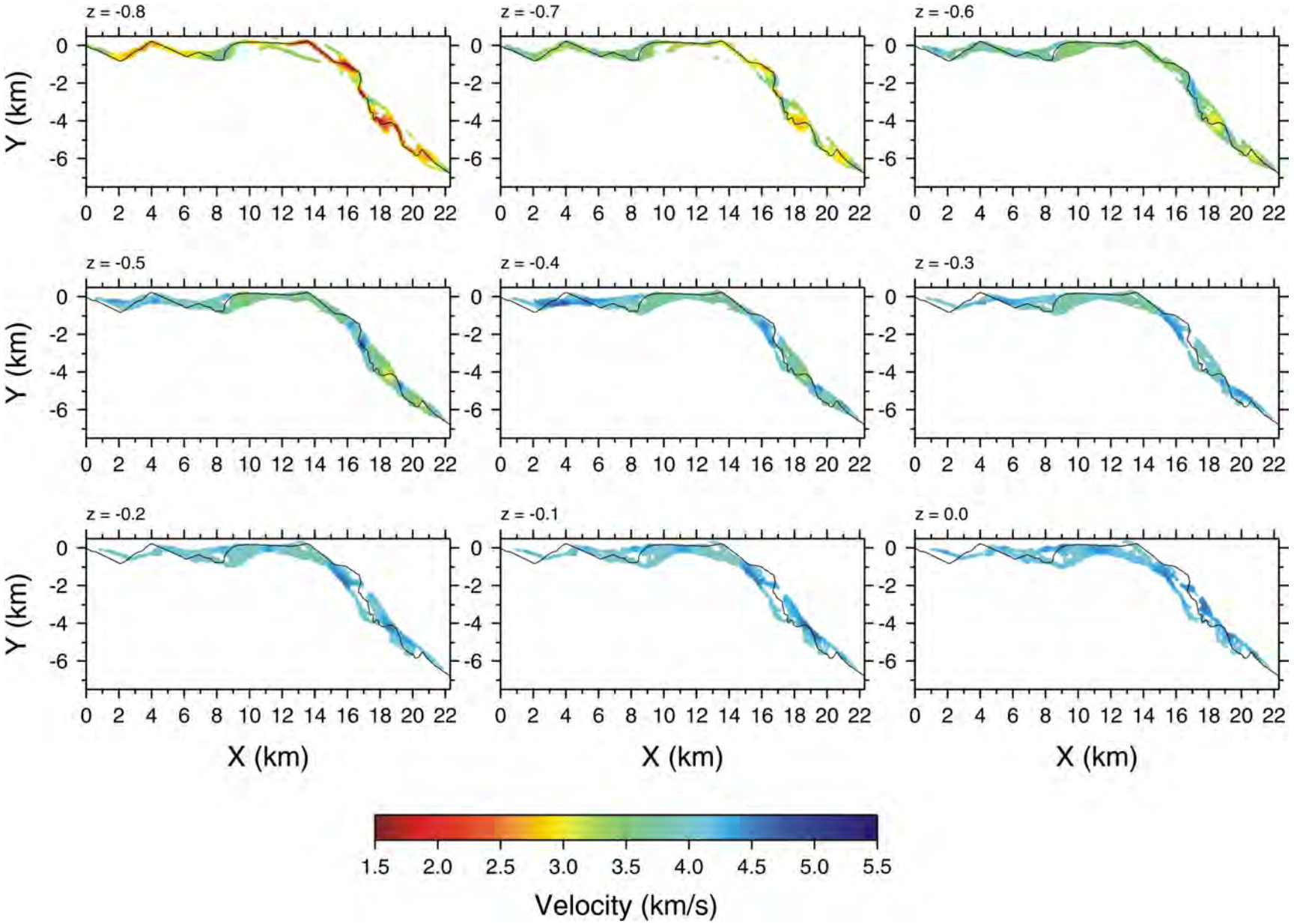

Figure 7. Horizontal slices of the velocity model for line 2008-11 at depth intervals of 100 m, showing localized low-velocity anomalies at the eastern end of the line. The top left slice is from the shallowest depth and the bottom right slice is from the deepest depth.

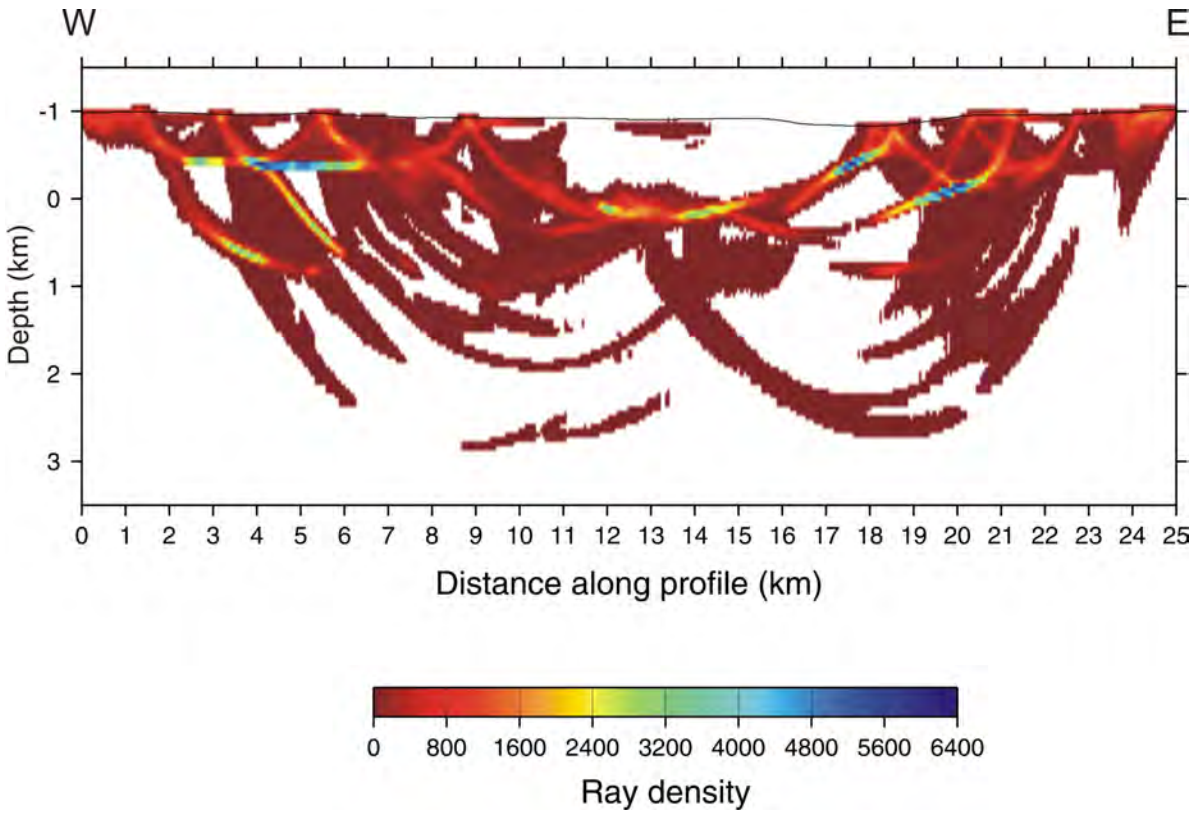

Figure 8. Ray density along line 2008-11, showing rays penetrating 3.5 km below the surface. The ray distribution is generally very irregular, with alternating high- and low-density zones, and occasionally absent ray coverage. Depths are measured relative to mean sea level.

Conclusions and Future Work

Preliminary 3-D inversions of first arrivals from two 2-D crooked reflection seismic lines recovered the long-wavelength velocity variation. Intensive testing showed that the starting velocity models for the inversion of the two lines should differ because of lateral variations in the thickness and seismic velocities of near-surface volcanic rocks and the underlying rocks. The starting velocity models for both lines correlate well with results from tomographic modelling of the Canadian Hunter data (Hayward and Calvert, 2009). In particular, line 2008-15, shot across Eocene Endako and Ootsa Lake rocks, has a starting velocity value of 3.3 km/s, consistent with the previously determined velocity range of 3.0–4.2 km/s; and line 2008-11, shot across mostly Neogene rocks from the Chilcotin Group, has a starting velocity value of 3.1 km/s, similar to the determined typical range of 2.4–3.0 km/s for this interval.

Some correlation of the near-surface modelled velocity with the known surface geology has been observed for line 2008-11. Shallow horizontal slices of the velocity model for this line show a correspondence between the volcanic cover and localized high-velocity anomalies of 3.5 km/s, and between sedimentary deposits and low-velocity anomalies of 2.5 km/s. In contrast, no strong relationship has been observed for line 2008-15, suggesting either a change in the layer thickness of the Eocene Endako and Ootsa groups, or that the rocks from the two groups may be distinguished based on velocity.

Appraisals of the velocity models were obtained using ray-density maps. We found that, although the 3-D method cannot achieve the ray density and uniformity of a 2-D experiment, 2-D inversion of crooked-line data has the potential to produce velocity and depth errors due to out-of-plane effects that are not addressed by a 2-D tomographic inversion. For line 2008-15, the recovered velocity model is most reliable at depths of less than 0.8 km. In contrast, the recovered velocities beneath line 2008-11 are less well constrained due to more complicated out-of-plane propagation.

Future work in this area will focus on refining the current velocity models and developing detailed velocity models that will constrain near-surface rock types, particularly beneath the volcanic cover, and permit a more detailed interpretation of the seismic-reflection data than is currently possible.

Acknowledgments

This project is being funded by Geoscience BC. We thank C. Zelt for providing the first-arrival tomography code. All velocity and ray-density figures were created with GMT. We also thank the reviewers—C. Sluggett, B. Davie and H. Isaac—for their excellent observations and suggestions that helped to improve the final manuscript.

References

Calvert, A.J. and Hayward, N. (2009): Seismic imaging beneath the volcanic rocks of the Nechako Basin, British Columbia; Canadian Society of Petroleum Geologists (CSPG)–Canadian Society of Exploration Geophysicists (CSEG)–Canadian Well Logging Society (CWLS), Annual Convention, 2009, Expanded Abstracts, p. 442–445, URL <http://www.cspg.org/conventions/abstracts/2009abstracts/060.pdf> [November 2010].

Calvert, A.J., Hayward, N., Smithyman, B.R. and Takam Takougang, E.M. (2009): Vibroseis survey acquisition in the central Nechako Basin, south-central British Columbia (parts of NTS 093B, C, F, G); *in* Geoscience BC Summary of Activities 2008, Geoscience BC, Report 2009-1, p. 145–149, URL <http://www.geosciencebc.com/i/pdf/SummaryofActivities2008/SoA2008-Calvert_original.pdf> [November 2010].

Ferri, F., and Riddell, J. (2006): The Nechako Basin project: new insights from the southern Nechako Basin; *in* Summary of Activities 2006, BC Ministry of Energy, p. 89–124.

Fliedner, M.M., White, R.S. and Smallwood, J.R. (1998): Seismic velocity structure of basalt flows (abstract); Society of Exploration Geophysicists (SEG), Annual Meeting, 1998, Expanded Abstracts, v. 17, p. 1178–1181, doi:10.1190/1.1820102.

Hannigan, P., Lee, P.J., Osadetz, K.G., Dietrich, J.R. and Olsen-Heise, K. (1994): Oil and gas resource potential of the Nechako-Chilcotin area of British Columbia; BC Ministry of Forests, Mines and Lands, GeoFile 2001-6, 38 p.

Hayes, B.J.R. and Fattahi, S. (2002): The Nechako Basin—frontier potential close to home (abstract); Canadian Society of Petroleum Geologists (CSPG), Annual Meeting, 2000, Extended Abstracts, URL <http://www.cspg.org/conventions/abstracts/2002abstracts/extended/051S0118.pdf> [November 2010].

Hayward, N., and Calvert, A.J. (2009): Eocene and Neogene volcanic rocks in the southeastern Nechako Basin, British Columbia: interpretation of the Canadian Hunter seismic reflection surveys using first-arrival tomography; Canadian Journal of Earth Sciences, v. 46, p. 707–720, doi:10.1139/E09-041.

Hole, J.A. and Zelt, B.C. (1995): Three-dimensional finite-difference reflection traveltimes; Geophysical Journal International, v. 121, p. 427–434.

Lafond, C.F., Kaculini, S. and Martini, F. (1999): The effects of basalt heterogeneities on seismic imaging of deeper reflectors (abstract); Society of Exploration Geophysicists (SEG), Annual Meeting, 1999, Expanded Abstracts, v. 18, p. 1433–1436, doi:10.1190/1.1820786.

Riddell, J. (2009): Evaluation of potential petroleum systems in the Nechako Basin; *in* Geoscience Reports 2009, BC Ministry of Energy, p. 53–63.

Vidale, J.E. (1990): Finite-difference calculation of traveltimes in three dimensions; Geophysics, v. 55, no. 5, p. 521–526, URL <http://earthweb.ess.washington.edu/vidale/Reprints/Geophysics/Vidale_Geophys_1990.pdf> [November 2010].

Zelt, C.A. and Barton, P.J. (1998): Three-dimensional seismic refraction tomography: a comparison of two methods applied to data from the Faeroe Basin; Journal of Geophysical Research, v. 103, no. B4, p. 7187–7210.

Zelt, C.A., Azaria, A. and Levander, A. (2006): 3D seismic refraction traveltime tomography at a groundwater contamination site; Geophysics, v. 71, no. 5, p. H67–H78, URL <http://eps.mcgill.ca/~courses/c435/Seismic-GPR-papers/Zelt-etal-3Drefract.pdf> [November 2010].